Smart Structures and Systems, *Vol. 17, No. 4 (2016) 541-557*
DOI: http://dx.doi.org/10.12989/sss.2016.17.4.541

Seismic performance of prefabricated bridge columns with combination of continuous mild reinforcements and partially unbonded tendons

Koem Chandara*, Shim Chang-Su[a] and Park Sung-Jun[b]

Department of Civil Engineering, Chung-Ang University, Seoul 156-756, Korea

(Received November 19, 2015, Revised February 12, 2016, Accepted February 17, 2016)

Abstract. Prefabricated bridge substructures provide new possibility for designers in terms of efficiency of creativity, fast construction, geometry control and cost. Even though prefabricated bridge columns are widely adopted as a substructure system in the bridge construction project recently, lack of deeper understanding of the seismic behavior of prefabricated bridge substructures cause much concern on their performance in high seismic zones. In this paper, experimental research works are presented to verify enhanced design concepts of prefabricated bridge piers. Integration of precast segments was done with continuity of axial prestressing tendons and mild reinforcing bars throughout the construction joints. Cyclic tests were conducted to investigate the effects of the design parameters on seismic performance. An analytical method for moment-curvature analysis of prefabricated bridge columns is conducted in this study. The method is validated through comparison with experimental results and the fiber model analysis. A parametric study is conducted to observe the seismic behavior of prefabricated bridge columns using the analytical study based on strain compatibility method. The effects of continuity of axial steel and tendon, and initial prestressing level on the load-displacement response characteristics, i.e., the strain of axial mild steels and posttensioned tendon at fracture and concrete crushing strain at the extreme compression fiber are investigated. The analytical study shows the layout of axial mild steels and posttensioned tendons in this experiment is the optimized arrangement for seismic performance.

Keywords: prefabricated bridge pier; partially unbonded tendon; nonlinear analysis; seismic performance

1. Introduction

Construction industry requires more innovative design and construction technologies to improve current practices. Prefabrication of structures has recently attracted much attention from bridge engineers. Prefabrication of bridge substructures is essential for accelerated bridge construction. Precast segmental columns may have bonded or unbonded posttensioning systems according to their required structural performance. These applications still lack of knowledge of seismic design parameters according to the required performance.

*Corresponding author, Graduate School Student, E-mail: koemchandara@cau.ac.kr
[a] Professor., E-mail: csshim@cau.ac.kr
[b] Ph.D. Student, E-mail: sakano@nate.com

http://www.techno-press.org/?journal=sss&subpage=8 ISSN: 1738-1584 (Print), 1738-1991 (Online)

Currently, many research works on precast columns has constantly been accomplished in experiments and analysis. Billington (2001) improved the alternative substructure system by using precast system. They found that prefabricated application increased the substructure durability. Experiment of small-scale experiment precast columns was conducted by Billington and Yoon (2004). Hysteretic energy dissipation of precast columns was improved until exceeding 3% to 6% of drift ratio. Hewes (2002) completed the experiment on the performance of unbonded post-tensioned precast concrete segmental bridge columns under lateral earthquake loading. The precast columns withstood without significant or sudden loss of strength up to 4.0% drift ratio.

Chiewanichakorn and Aref (2006) implemented the finite element simulation of seismic response of the precast concrete segmental columns. The analysis schemes were developed considering the interface between segments with opening-closing under cyclic loading. FEM analysis was able to capture the actual behavior of this new structural system. Ou (2007) has done the experiment and pushover analysis on segmental precast unbonded posttensioned bridge columns with a hollow cross section. They found that the enhancement of column hysteretic energy dissipation was improved. They also did large-scale experimental investigation and showed effectiveness of unbonded ED (energy dissipation) bar to improve seismic performance. Shim (2008) conducted the experiment on six precast piers to evaluate on seismic performance of precast segmental bridge piers with a circular solid section. The prefabricated composite columns have also been tested with cyclic load and observed the seismic performance with low steel ratio of less than 4% (Shim *et al.* 2008). By increasing the steel ratio, the plastic deformation and its energy absorption capacity increased after exceeding its maximum strength. A hybrid sliding-rocking posttensioned segmental bridge system was extensively investigated by Sideris *et al.* (2014a,b, 2015). Internal unbonded posttensioning and slip-dominant joints were used to provide self-centering and energy dissipation. Shim et al. (2011) accomplished the extensive tests to observe the cyclic behavior of prefabricated circular composite columns with low steel ratio. Higher prestressing gave greater flexural strength to the composite columns with prestressing and better energy absorption capacity.

A prefabricated composite column with embedded circular tubes showed ultimate reflected the increasing Ultimate strength and energy absorption capacity (Shim *et al.* 2012). Nikbakht *et al.* (2014) implemented a numerical study on seismic response of self-centering precast segmental columns at the difference of posttensioning forces. The higher initial prestressing strand levels reflected greater initial stiffness and strength, but show a higher stiffness reduction at large drifts. Effective prestressing stress and location of axial steels should be designed to have optimal plastic behavior at target lateral deformation of the columns (Shim *et al.* 2015). In design consideration, Shim (2015) suggested the design of precast column by applying the combination of axial steels was considered such as posttensioned tendons and continuous reinforcing steels.

In this paper, an experimental program was conducted to investigate seismic performance of precast segmental bridge columns with combination of partially unbonded tendons and continuous mild reinforcements crossing precast joints. Geometry of the precast joints was enhanced. Essential design parameters for seismic behavior of the precast columns were discussed based on the cyclic tests.

2. Experimental program

2.1 Test specimens

A laboratory testing program was conducted to assess the static and seismic performance of the proposed prefabricated bridge pier system under cyclic loading. As shown in Fig. 1, to prove the effect of parametric design, two prefabricated bridge columns specimens were tested. The design specimens consisted of two segments with 800 mm diameter circular sections. The footing segment was fixed to the strong floor. The effective length from the loading point to plastic hinge point is 2750 mm. Aspect ratio of the columns were 3.44, which leads to flexural failure.

The fabrication procedure of the precast pier system is illustrated in Fig. 2. The fabrication contains two circular-section segments and base footing for the prefabricated columns specimen. In order to ensure the accuracy of geometry control, 3D models for the precast segments and formworks were developed. The mild reinforcing steel bar was connected with coupler, and the design jacking force was introduced by prestressing at the anchorage of the footing.

A concrete footing segment had details of the tendon anchorages at side surfaces, and geometry control of the location of the ducts and longitudinal reinforcing bars was crucial for assembly as shown in Fig. 2(a). The footing reinforcements consisted of 22 mm diameter at spacing 200 mm in both directions. The prestressing tendon and anchorage were placed on both side surface of footing. The anchorages were placed at 120 mm height from the bottom most of the footing. To ensure the anchorage zone, the spiral confinements were reinforced the compression zone. Concrete parts such as footing, segment 1 and segment 2 were prefabricated separately. To improve matched segment, Fig. 2(b) shows the confining reinforcement cage arranging with prestressing tendon and continuous axial steel ducts. The steel formworks were fabricated to ensure the circular section of concrete as well as the alignment of prestressing tendon and axial steel ducts. Each reinforcement cage for each part was tied and placed on the casting bed, which is covered by the steel formworks. The 55-mm-diameter corrugated tubes were placed in reinforcement cages to create ducts of the non-prestressing and prestressing steels. Prestressing tendons and non-prestressing steels were aligned throughout the segments during the stacking stage of the construction process.

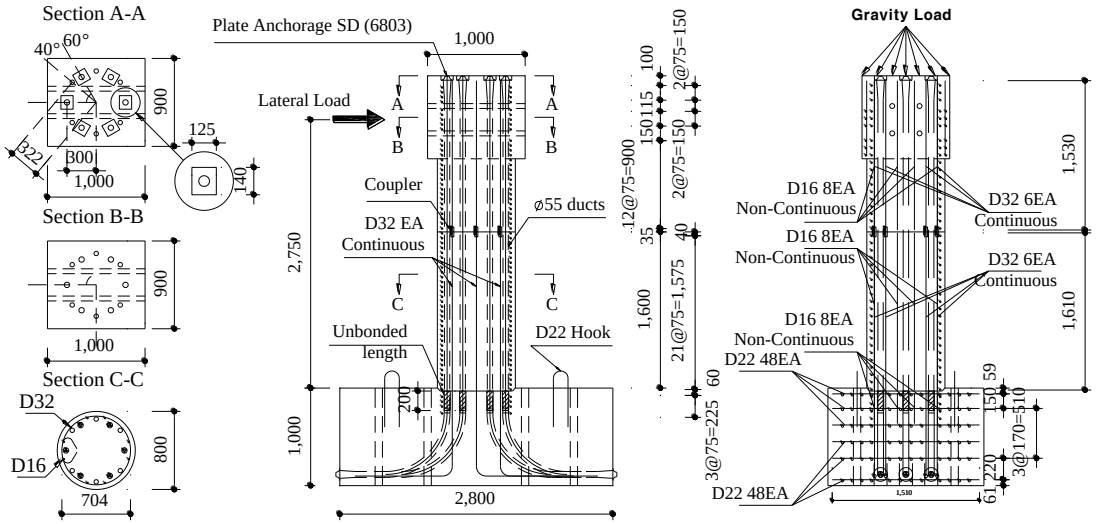

Fig. 1 Prefabricated bridge pier details

The tendon jacking phase was conducted on both sides of the footing. Based on a design against slip failure of the plastic hinge connection, the special-detailing shear key were proposed at the footing-the first segment connection. The shear key was detailed with 30 mm x 30 mm chamfer shape, where the segment1 was embedded into the footing as illustrated in Fig. 2(c). In this experiment, the partially unbounded length of 200 mm prestressing tendon was proposed in order to mitigate the stress concentration at the plastic hinge connection. To ensure partially unbonded, each prestressing tendon was wrapped to envelop with plastic tape as shown in Figure 2(d). Axial prestressing was introduced sequentially with symmetric order. The measurement of initial prestressing was performed by pressure gauge of a hydraulic jack and elongation of the tendon.

(a) Reinforcement of footing

(b) Transverse reinforcement for segment segments

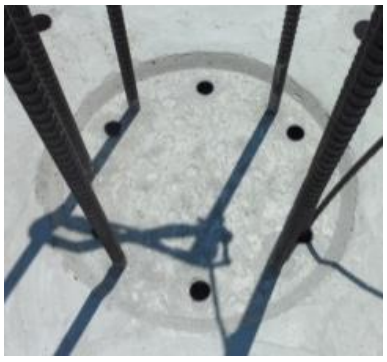

(c) Joint between a segment and footing

(d) Debonding of tendon

Fig. 2 Fabrication procedure

The details of test specimens are summarized in Fig. 1. The diameter of 800 mm was selected for both test specimens PT1-TD and PT2-TD. The experiment was conducted to investigate the initial stress level of prestressing tendon and the effect of partially unbonded length on prefabricated bridge piers based on the load-displacement response of the columns. Each specimen consisted of a 2800 mm x 1600 mm x 1000 mm footing, and two 800 mm diameter segments. The longitudinal reinforcement in each column contained both non-prestressing and prestressing steel. The non-prestressing steel of 6 - 32 mm diameter 471-MPa-yield-strength rebars were bonded continuously along entire columns.

The compressive strength of concrete, f'_c, was taken as 41.5 MPa. The final details of both specimens are shown in Table 1. The partially unbonded prestressing steel consists of 6 – 15.2 mm diameter of the wire stands ASTM A779 Grade 270 (1860 MPa) low-relaxation with total cross-section area of 2497 mm^2. The yield strength of posttensioned tendon is 1640 MPa, which was measured at 0.1% residual elongation. The partially debonding length at the footing, L_t, 200 mm. Accelerated damage of concrete occurred when the buckling failure of reinforcement had occurred. The discontinuous non-prestressing reinforcement of 8 – 16 mm diameter with yield strength of 479 MPa at the joint played as an important function to delay the rapid damage. The columns were confined by the transverse reinforcement of 16 mm diameter with yield strength of 479 MPa rebar at 75mm spacing.

One of the main parametric tested in this research work was the effective prestressing level. Based on current bridge design standard codes (AASHTO LRFD 2012 Section 5.9.3), the allowable effective prestressing level at limit state after all loses is 80 percent of yield strength of prestressing posttensioned tendon. In order to observe the effect of effective prestressing level on the partially unbonded bridge columns, the effective prestressing tendons were provided with different of 84.45% and 53.60% of yield strength of posttensioned tendons for specimen PT1-TD and PT2-TD, respectively.

2.2 Test setup

Quasi-static tests are conducted to evaluate the cyclic respose of the partially unbonded bridge columns. Since all the tested prefabricated bridge columns were cantilevers, the test setup was design for testing column-footing assemblage subjected to a combination of axial load and cyclically applied lateral load. The two loading system are applied independently to the specimens. As shown in Figs. 3(a)-3(b), the constant axial load of 1000 kN was applied to the top surface of the columns, which calculated from the equation $P/A_g f'_c = 5\%$. This was done by pre-stressing a pair of high-strength steel rods against the reinforced deep floor via the loading frame.

Table 1 Test program of partially unbonded bridge columns

Specimen	Number of Tendon	Longitudinal reinforcement	Steel ratio (%)	Transverse reinforcement	f_{pe} (MPa)	f_{pe}/f_{py} (%)	Partially unbonded length L_{au} (mm)	$P/A_g f'_c$ (%)
PT1-TD	6⌀15.2 mm 3-wire strands	6⌀32 mm	1.45	⌀16 mm@75 mm	1385	84.45	200	5
PT1-TD					879	53.60		

The axial force level was chosen by considering the actual force experienced by bridge columns, which is commonly 10% of axial strength. A specimen was secured in place by post-tensioning its footing to the strong reinforced concrete floor.

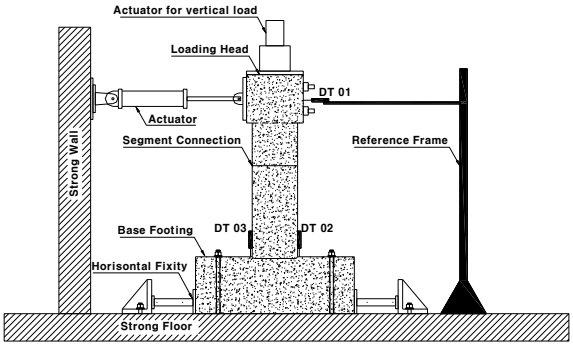

(a) Schematic test setup

(b) Laboratory test setup

Fig. 3 Experimental test Setup

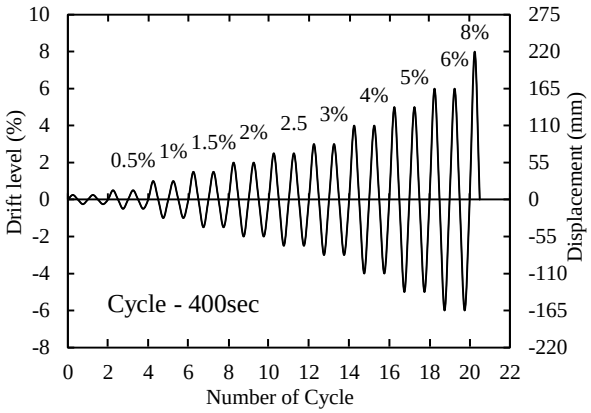

Fig. 4 Load protocol used for PT1-TD and PT2-TD

Repeated lateral forces were simultaneously applied to the column by a hydraulic actuator mounted to the strong reinforced concrete walls. The cyclic test was carried out in displacement method as shown in Fig. 4. The drift levels are used to represent the displacement controlled test, which started at ±0.25% and subsequently increased to ±0.50%, ±1.00%, ±1.50%, ±2.00%, ±2.50%, ±3.00%, ±4.00%, and so on, stopping at point of failure. The drift level is defined as the ratio of input displacement to the column height.

2.3 Test results

As shown in Figs. 5(a)-5(b), all the tested bridge colums exhibited ductile flexural reponse up to the maximum imposed drift of 8%. Both specimens showed the flexural failure. From the Fig. 5, monotonic response of prefabricated bridge pier can be observed in the interval of 0.5% to 8.0 % drift level. Before exceeding the drift ratio of 2.5%, both specimens showed the similar behavior. However, the specimen PT1- TD has deceased its stiffness from a drift level of 2.5% to 4.0% due to concrete crushing. Different initial stress levels of prestressing tendon significantly have the influence on ductile behavior of segmental prefabricated bridge piers. With 84.45%f_{py} initial prestressing stress level, strength degradation of PT1-TD had occurred earlier than PT2-TD. The peak strength of PT1-TD for push direction and pull direct are 558 kN and 575 kN, respectively. Since the strength of PT1-TD noticeably reduced, the ductile behavior of the column was governed by higher initial prestressing level.

The behavior of PT2-TD becomes stable respecting to the low-stress level of prestressing tendons with 45%fpu, and it postponed its stability until the 5.0% drift level. This specimen PT2-TD performs higher deformation regarding the higher bearing capacity. In push direction, PT1-TD is capable to resist the peak strength of 542 kN, while resistance in pull direction is 573 kN. Even though the reduction of bearing capacity of the column at a drift level of 6.0%, the strength of the column remained higher than the ultimate strength.

3. Analysis

3.1 Moment-curvature analysis

The analysis employed in this study to validate the research work on experiment of the partially unbonded prefabricated bridge piers is derived from the moment-curvature analysis. It is assumed that the compatibility between tendon and mild steel is valid. This basic theory is also applicable for nonlinear analysis of prefabricated bridge pier, and the required basic assumption for strain compatibility theory are (1)The stress distribution in the compression zone of concrete can be defined by integration of confined and unconfined concrete stress-strain model as depicted in Fig. 8; (2) the concrete strain is assumed linearly (plane sections normal to axis remain plane after bending); (3) the resistance of concrete in tension is neglected to allow the opening at the connection at base footing as shown in Fig. 6; (4) The maximum compressive strain of unconfined concrete at failure reaches the strain of 0.0035, while maximum compressive strain of confined concrete at failure reaches the fracture strain of first transverse steel.

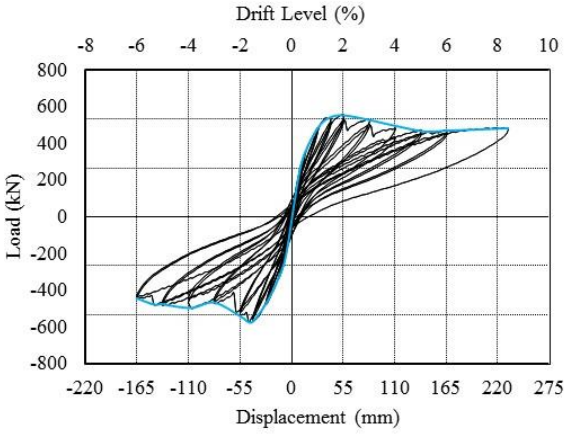

(a) PT1-TD

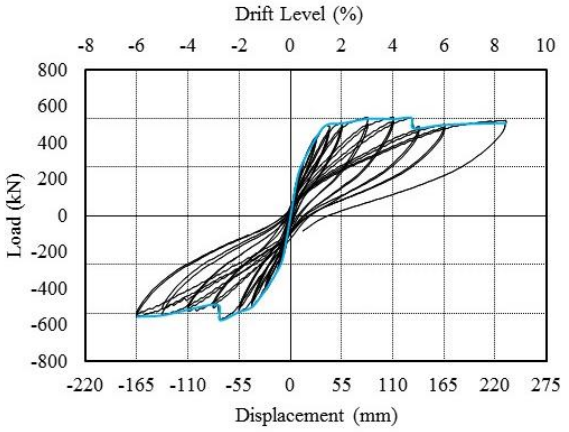

(b) PT2-TD

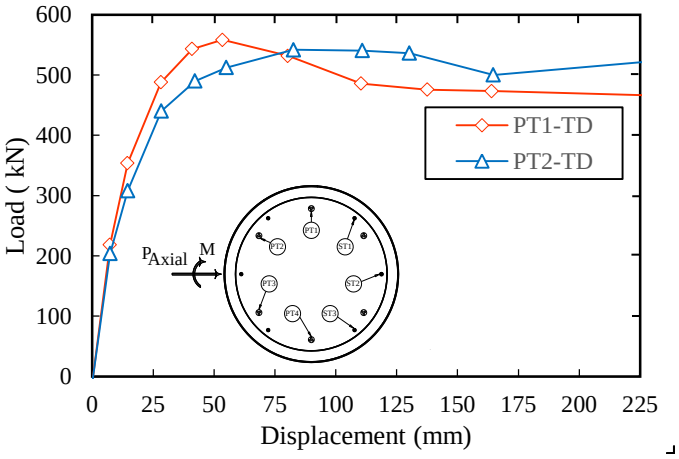

(c) Envelop curves

Fig. 5 Global behavior of partially unbonded prefabricated bridge columns

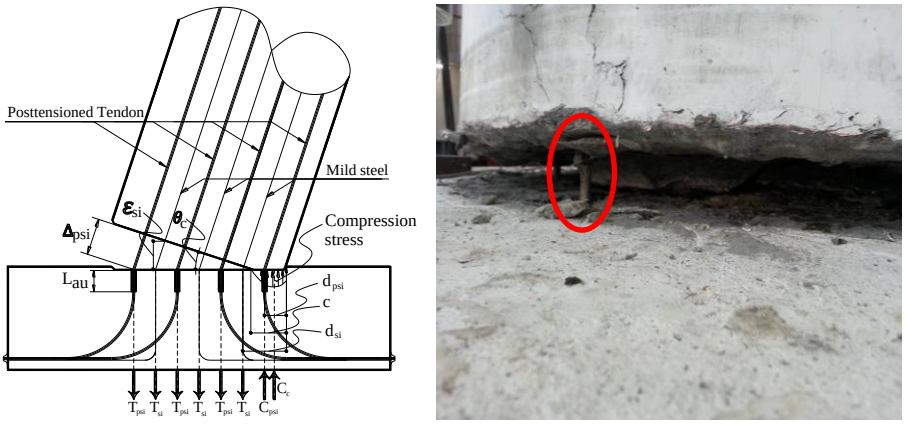

Fig. 6 The schematic diagram of base joint connection

Owing to the existence of the segmental connection, the column rotation was concentrated at the joint as shown Fig. 6. To exhibit good performance in term of lateral capacity and stress concentration reduction, the partially unbonded posttensioned tendons were placed at base footing with 200 mm unbonded length. Since the opening at joint occurs, the elongation of posttensioned tendon produces the additional strain to the tendon. Bu (2015) has done the cyclic loading test on unbonded and boned posttensioned precast segmental bridge columns with circular section, which the method of considering the unbonded system was described. Similarly, effect of partially unboned posttensioned tendon additional strain on strain from compatibility. The additional strain of partially unbounded posttensioned tendon, $\Delta\varepsilon_{psi}$, is computed as

$$\Delta\varepsilon_{psi} = \frac{\Delta_{psi}}{L_{eu}} \tag{1}$$

Where Δ_{psi} is the elongation of the posttensioned tendon after joint opening; L_{eu} is the partially unbonded length of posttensioned tendon as depicted in Fig. 6.

Applying strain compatibility method as shown in Fig. 8, the posttensioned tendon has total strain as combination of effective prestressing, axial strain from the axial force, and additional strain from the partially debonding effect. The total strain of tendon at segmental joint can be derived as

$$\varepsilon_{psi} = \varepsilon_{pe} + \frac{P}{A_c E_c} + \Delta\varepsilon_{psi} \tag{2}$$

The theoretical moment-curvature curve for posttensioned prefabricated bridge piers' sections with axial load and lateral load can be derived on the basic assumptions similar to those used for estimation of flexural strength. The curvatures of the section under axial load and lateral load can be obtained from the requirement of strain compatibility and equilibrium of forces. The axial load P and bending moment M at any loading stage carried out by the reference axis going through the center of a section are found by integrating the stresses over the section.

$$\mathrm{P} = \int_{\frac{D_c}{2}-c}^{\frac{D_c}{2}} \sigma_c dA_c + \int_{\frac{D_c}{2}-c}^{\frac{D_c}{2}} \sigma_{cc} dA_{cc} + \sum_{i=1}^{n}(\sigma_{si} - \sigma_{cci})\ A_{si} + \sum_{i=1}^{n}\left(\sigma_{psi} - \sigma_{cci}\right)\ A_{psi} \tag{3}$$

$$M = \int_{\frac{D_c}{2}-c}^{\frac{D_c}{2}} \sigma_c x dA_c + \int_{\frac{D_c}{2}-c}^{\frac{D_c}{2}} \sigma_{cc} x dA_{cc} + \sum_{i=1}^{n} (\sigma_{si} - \sigma_{cci}) A_{si} \left(\frac{D_c}{2} - d_{si}\right) + \sum_{i=1}^{n} (\sigma_{psi} - \sigma_{cci}) A_{psi} \left(\frac{D_c}{2} - d_{psi}\right) \quad (4)$$

Where D_c is the diameter of circular bridge piers; σ_c and σ_{cc} are the stress of unconfined and confined concrete as shown in Fig. 9; dA_c and dA_{cc} are the incremental subarea of cover concrete and core concrete; σ_{si} and σ_{psi} are the stress level at the layer *i* of mild steels and posttensioned tendons; A_{si} and A_{psi} are the nominal areas of mild steel and posttensioned tendon at layer *i*; d_{si} and d_{psi} the depth from extreme compressive fiber to center of mild steel and posttensioned tendon at layer *i*.

The curvature is given by similarity as

$$\theta_c = \frac{\varepsilon_{max}}{c} \quad (5)$$

Where ε_{max} is the maximum strain value at the extreme compressive fiber of section, and c is the neutral axis of section.

The key steps to be followed in moment-curvature determination using strain compatibility method and equilibrium forces are summarized as (1) divide the concrete section into as many as with small thickness (the more small thickness gives the accuracy) as shown in Fig. 7; (2) Assume initial curvature in elastic range θ_{ci}; (3) Assume strain at the extreme compressive fiber ε_{max}, and compute the location of neutral axis as Eq. (6); (4) from similar triangles of strain diagram, evaluate strain magnitude at each layer assuming linear distributed as shown in Fig. 8. The strain of concrete, mild steel and posttensioned tendon at layer i are evaluated.

$$c = \frac{\varepsilon_{max}}{\theta_c} \quad (6)$$

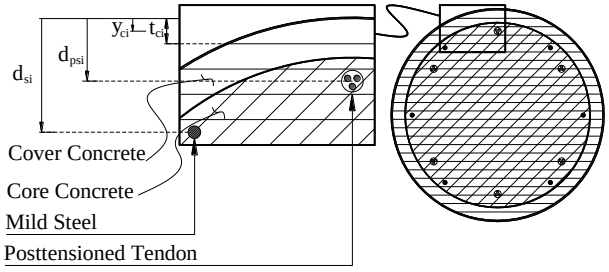

Fig. 7 subdivision of cross section into small-thickness subareas

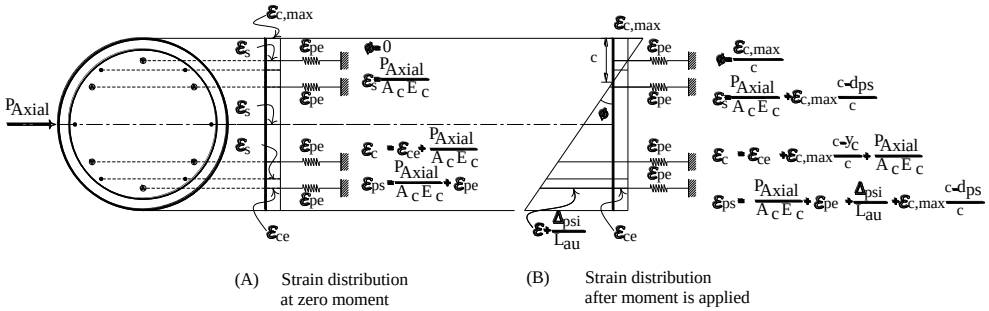

Fig. 8 The Strain and strain assumed in analysis

3.2 Material model

3.2.1 Concrete

The concrete material model used in this analytical study was adopted based on European standard (pnEN 1992-1-1). For a given concrete characteristic compressive strength f_c' the stress-strain model for concrete were derived for nonlinear structural analysis as shown in Fig. 9(a). The unconfined concrete jumps its strength to be a confined concrete because of the effective lateral confining pressure and the confined effectiveness coefficient. The stress-strain curve is illustrated in Fig. 9(b).

3.2.2 Mild steel

The stress-strain model of mild steel reinforcement is idealized linearly as elastic region, plastic hardening region as shown in Fig. 10(a). The idealization stress-strain model is derived based on Eurocode code 2 (pnEN 1992-1-1).

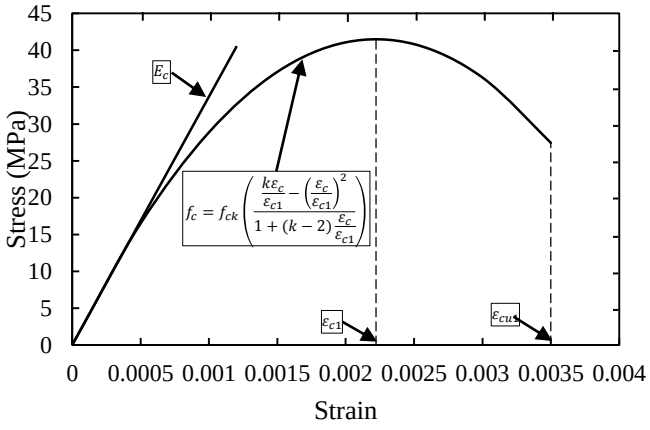

(a) Unconfined concrete

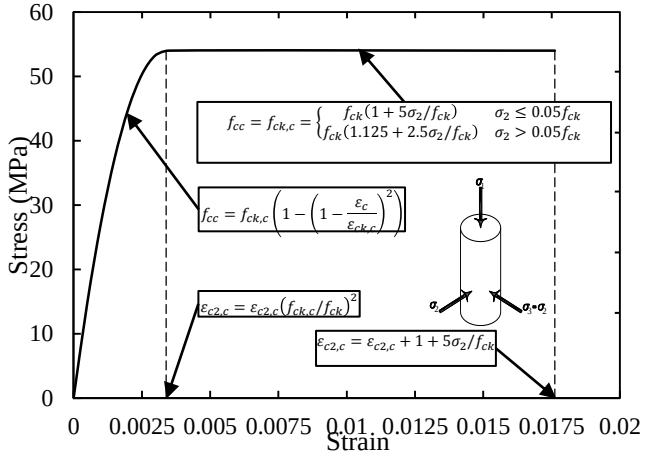

(b) Confined concrete

Fig. 9 Stress-strain model for concrete (prEN 1992-1-1)

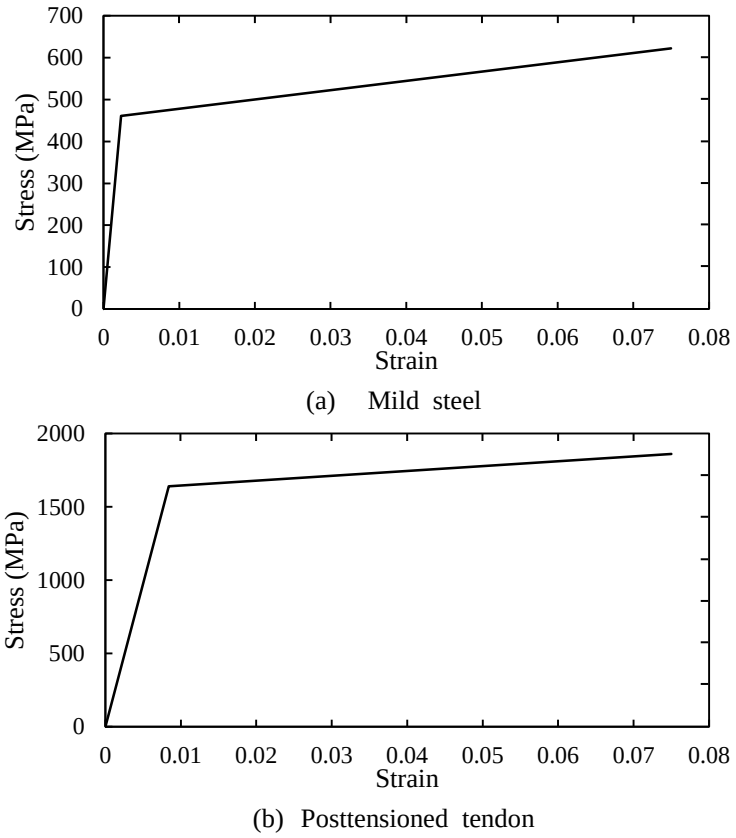

(a) Mild steel

(b) Posttensioned tendon

Fig. 10 Stress-strain model for axial reinforcement (prEN 1992-1-1)

3.2.3 Posttensioned tendon

The posttensioned tendon is selected as low-relaxation steel prestressing strands, complying with ASTM A 416. Strands can be supplied either bare, galvanized or epoxy-coated without any loss in strength including the wedge anchorage. For a maximum in corrosion protection we offer electrically isolated systems using polyethylene (PE) or polypropylene (PP) duct. A typical stress-strain relationship for the industry standard grade 270 strand is shown below in Fig. 10(b).

3.3. Analysis results and comparison

In order to validate the analytical study, the comparison of load-displacement curve from the experimental results and the moment-curvature analysis as shown in Figs. 11(a)-11(b). Since the nominal strength of material was used in the moment-curvature analysis, the strength resulting from analysis seems to be greater than the strength from the test approximately 3.1% and 7.3 % for PT1-TD and PT2-TD, respectively. With this range of difference, moment-curvature analysis can be utilized to conduct the parametric study on partially unbonded prefabricated bridge columns.

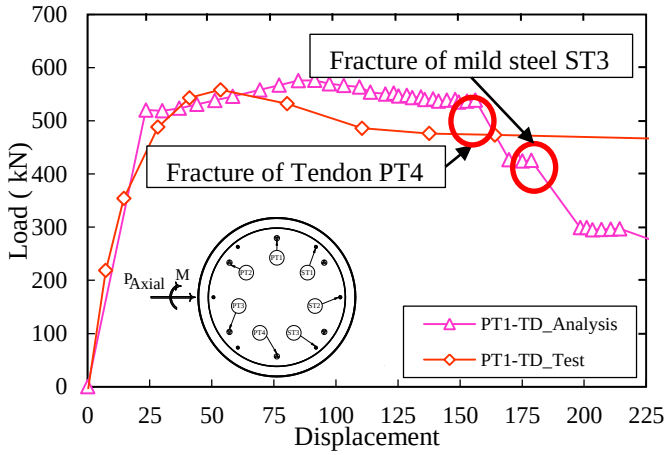

(a) PT1-TD

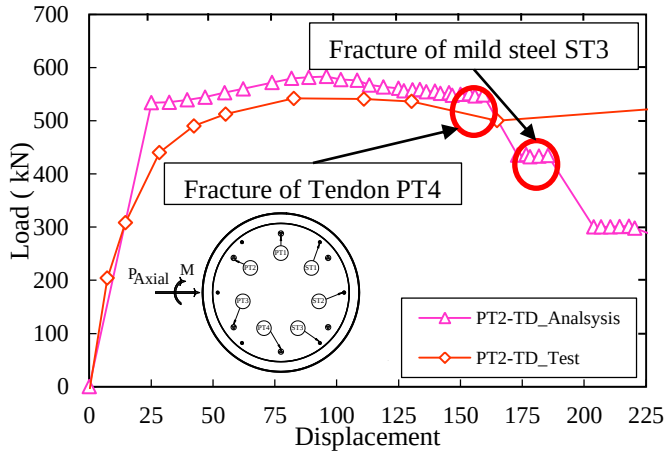

(b) PT1-TD

Fig. 11 Comparison of load – displacement curve

4. Parametric study

The analysis described above may be utilized to evaluate the complete moment-curvature analysis for partially unbonded prefabricated bridge columns for a given section. By conducting the moment-curvature analysis a given section of the prefabricated bridge columns, the effect of change in effective prestressing level can be studied based on comparison of load-displacement curve. In addition, the fracture and stress level of each material was investigated so that evaluate the structural response of partially unbonded prefabricated bridge columns. The given circular section of the prefabricated bridge column was reinforced with a combination between symmetric posttensioned tendons and non-prestressing mild steel. The nominal strength of materials model shown in Figs. 8 and 9 was utilized. The effective prestressing level selected to conduct the parametric study vary in 55%, 70%, and 80% of yield strength of posttensioning tendon. The section destails is exactly same to the test specimens. The model used in moment-curvature

analysis named as PT55-TD, PT70-TD, PT80-TD, which corresponds to effective prestressing level of 55%, 70%, and 80% of yield strength of posttensioned tendon, respectively.

4.1 Effect of variation in effective prestressing level

As shown in Fig. 12, load-displacement curves for the partially prefabricated bridge columns. In this study the amount of non-prestressing steel and posttensioned tendon as well as its nominal strength was kept constant, but effective prestressing levels were varied. In elastic range of behavior where the section is uncracked, the trends of response are same. At cracking stage, there is no significant change in bearing capacity, although effective prestressing level was increased. Since the posttensioned tendons was placed at deeper level than on prestressing steel, the tendon facture occurred earlier than non-prestressing steel fracture. At the time tendon fracture, there is still slightly different curvature in both strength and curvature.

The magnitude of strain of mild steel and tendon is changed according to the increase of curvature. Figs. 13(a) and13(b) shows the strain-curvature of mild steel and posttensioned tendon. The mild steel fractured at curvature of 0.00196, 0.0002, and 0.00019 for applied effective prestress level of 80%, 70% and 55% of yield strength of tendon, respectively. Similarly, the curvature of 0.000164, 0.00016 and 0.00016 is the curvature at fractures of posttensioned tendon. Based on strain data, it still shows that there is small difference, however the wide range of effective prestressing level was applied.

The stress state of posttensioned tendon yield or fracture earlier depends on the applied effective prestressing level. Fig. 14 shows the stress-curvature curve of tendon. With applying varried effective prestressing level of 30% shows the earlier yield of tendon occured approximately 10.4% in case of higher prestressing level was applied. İnversely, for the section applied with lower prestressing level postponed its fracture time.

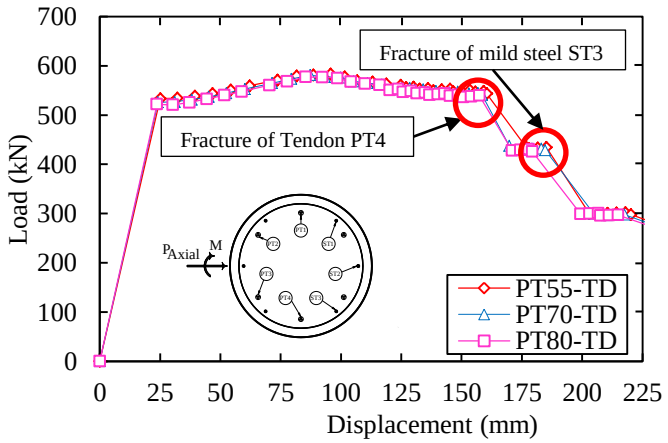

Fig. 12 Load-displacement curve

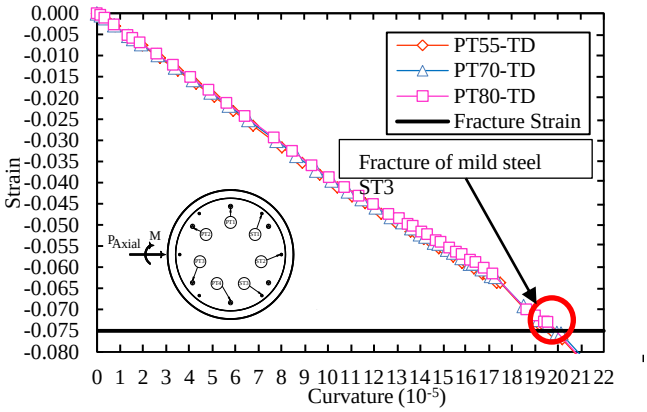

(a) Mild steel strain

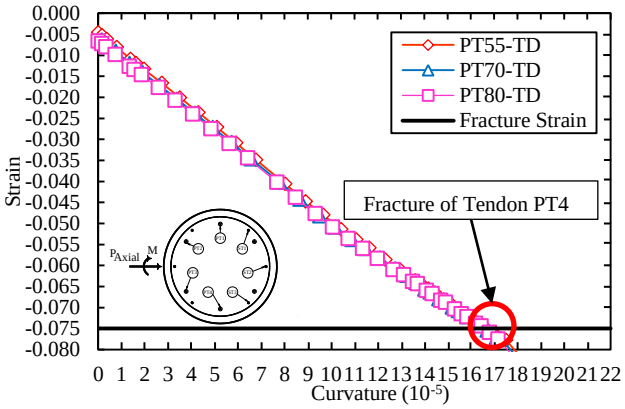

(a) Posttensioned tendon strain

Fig. 13 Strain – curvature curves

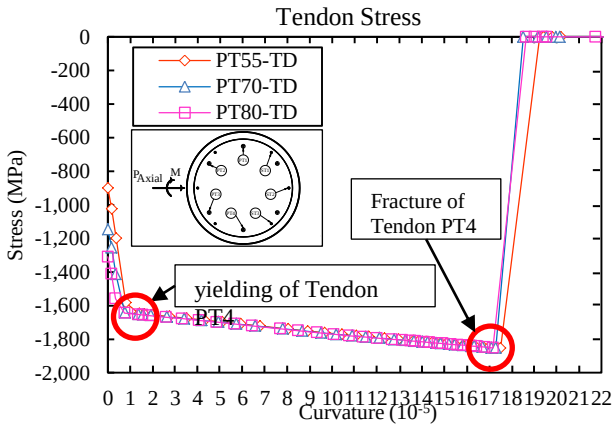

Fig. 14 Stress-curvature curve of posttensioned tendon

5. Conclusions

Through quasi-static test and analytical study, the structural response of partially unbonded prefabricated bridge columns was investigated. The following conclusions are made for performance of prefabricated bridge columns.

- The partially unbounded bridge columns performs ductile behavior and have the capability to resist large horizontal load up to drift ratio 8%. The bridge column behavior agreed with the earlier design concept, where the earlier strength degradation occurred on prefabricated bridge pier with higher prestressing level.
- The moment-curvature analysis can be utilized to estimate strength of partially unbounded bridge piers. The difference between test result and moment-curvature analysis is 3% and 7.7% for specimen PT1-TD and PT2-TD, respectively.
- Even though the variation in effective prestressing level of 25%, the curvature at yielding and fracture of tendon varies with 2%. The symmetric layout of posttensioned tendon and axial non-prestressing shows that maximum allowable prestressing level can be applied up to 80% of yield strength of tendon.

Acknowledgments

This research was supported by a grant (13SCIPA01) from Smart Civil Infrastructure Research Program funded by Ministry of Land, Infrastructure and Transportation (MOLIT) of Korea government and Korea Agency for Infrastructure Technology Advancement (KAIA).

References

AASHTO. (2007), AASHTO LRFD bridge specification (4th Ed.).

Billington, S., Barnes, R. and Breen, J. (2001), "Alternate substructure systems for standard highway bridges", *J. Bridge Eng.- ASCE*, **6**(2), 87-94.

Billington, S. and Yoon, J. (2004), "Cyclic response of unbonded posttensioned precast columns with ductile fiber-reinforced concrete", *J. Bridge Eng. - ASCE*, **9**(4), 353-363.

Bu, Z.Y. and Ou, Y.C. (2013), Simplified Analytical Pushover Method for Precast .

Chiewanichakorn, M. and Aref, A. (2006), "Finite element simulations of seismic response of precast concrete segmental columns", *Struct. Cong.- ASCE*, 1-9.

Eurocode 2 (prEN 1992-1-1), "Design of reinforced concrete structure", CEN –European Committee for standardization.

Hewes, J.T. and Priestly, M.J.N. (2002), *Seismic design and performance of segmental precast concrete column*, Report No. SSRP-2001/25, University of California, San Diego, CA.

Moon, D.Y., Roh, H. and Cimellaro, G.P. (2015), "Seismic performance of segmental rocking column connection with NITI Martensitic SMA bars", *Adv. Struct. Eng*., **18**(4), 571-584.

Nikbakht, E., Rashida, K., Hejazib, K. and Osmana, S.A. (2014), "A numerical study on seismic response of self-centering precast segmental columns at different post-tensioning forces", *Latin Am. J. Solids Struct*., 864-883.

Ou, Y.C., Chiewanichakorn, M., Aref, A.J. and Lee, G.C. (2007), "Seismic performance of segmental precast unbonded posttensioned concrete bridge columns", *J. Struct. Eng. - ASCE*, **133**(11), 1636-1647.

Ou, Y.C., Wang, P.H., Chang, K.C. and Lee, G.C. (2010), "Large-scale experimental study of precast segmental unbonded posttensioned concrete bridge columns for seismic regions", *J. Struct, Eng. - ASCE*, **136**(3), 255-264.

Shim, C.S., Chung, C.S. and Kim, H.H. (2008), "Experimental evaluation of seismic performance of precast segmental bridge piers with a circular solid section", *Eng. Struct*., **30**(12), 3782-3792.

Shim, C.S., Chung, Y.S. and Han, J.H. (2008), "Cyclic response of Concrete-encased composite columns with low steel ratio", Structure and buildings, Proc. Of the institution of Civil Engineers, 161, Issue SB2, 2008, 77-89.

Shim, C.S., Chung, Y.S. and Yoon, J.Y. (2011), "Cyclic behavior of prefabricated circular composite columns with low steel ratio", *Eng. Struct*., **30**(11), 2525-2534.

Shim, C.S., Kim, D.W. and Kong, D. (2012), "Structural performance of precast segmental composite pier cap", *Proceedings of the 18th Congress of International Association for Bridge and Structural Engineering*.

Shim, C.S., Park, S.J, Lee, S.Y. and Keom, C. (2015), "Enhanced design of precast concrete columns by optimal axial steels", *Earthquake Resistant Engineering Structure X*, (152), 267-273

Shim, C.S., Lee, S.Y., Park, S.Y. and Koem, C. (2015), "Cyclic tests on prefabricated bridge piers", *Proceedings of the advances in structural Engineering and Mechanics (ASEM15)*.

Sideris, P., Aref, A.J. and Filiatrault, A. (2014a), "Quasi-static cyclic testing of a large-scale hybrid sliding-rocking segmental column with slip-dominant joints", *J. Bridge Eng. - ASCE*, **19**(10), 04014036.

Sideris, P., Aref, A.J. and Filiatrault, A. (2014b), "Large-scale seismic testing of a hybrid sliding-rocking Posttensioned segmental bridge system", *J. Struct, Eng. - ASCE*, **140**(6), 04014025.

Sideris, P., Aref, A.J. and Filiatrault, A. (2015), "Experimental seismic performance of a hybrid sliding-rocking bridge for various specimen configurations and seismic loading conditions", *J. Bridge Eng. - ASCE*, **20**(11), 04015009.